Current Optics and Photonics
Vol. 4, No. 4, August 2020, pp. 368-372

ISSN: 2508-7266(Print) / ISSN: 2508-7274(Online)
DOI: https://doi.org/10.3807/COPP.2020.4.4.368

Quantitative Label-free Terahertz Sensing of Transdermal Nicotine Delivered to Human Skin

Gyuseok Lee[1], Ho Namkung[1], Youngwoong Do[1], Soonsung Lee[1], Hyeona Kang[1], Jin-Woo Kim[1,2], and Haewook Han[1]*

[1]*Department of Electrical Engineering, Pohang University of Science and Technology, Pohang 37673, Korea*
[2]*Department of Biological and Agricultural Engineering and Institute for Nanoscience and Engineering, University of Arkansas, Fayetteville 72701, USA*

(Received May 18, 2020 : revised June 11, 2020 : accepted June 15, 2020)

We report the terahertz time-domain spectroscopy (THz-TDS) of transdermal drug delivery in human skin. The time evolution of transdermal nicotine delivery in nicotine patches was assessed by detecting the transmission coefficient of sub-picosecond THz pulses and using a semi-analytic model based on the single-layer effective medium approximation. Using commercial nicotine patches (Nicoderm CQ®, 7 mg/24 h), THz transmission coefficients were measured to quantitatively analyze the cumulative amounts of nicotine released from the patches in the absence of their detailed specifications, including multilayer structures and optical properties at THz frequencies. The results agreed well with measurements by conventional *in vitro* and *in vivo* methods, using a diffusion cell with high-performance liquid chromatography and blood sampling respectively. Our study revealed the ability of the THz-TDS method to be an effective alternative to existing methods for noninvasive and label-free assessments of transdermal drug delivery, showing its high promise for biomedical, pharmaceutical, and cosmetic applications.

Keywords : Terahertz spectroscopy, Nicotine, Transdermal drug delivery
OCIS codes : (300.6495) Spectroscopy, terahertz; (160.1435) Biomaterials

I. INTRODUCTION

Terahertz time-domain spectroscopy (THz-TDS) is a coherent spectroscopic and non-ionizing radiation technique that provides both amplitude and phase information, to assess the complex refractive index of a medium. It has offered high promise to probe low-frequency intermolecular vibrational dynamics of biomolecules, providing functional and structural information about biological materials [1, 2]. Recent advances in THz-TDS have opened up many opportunities in the fields of biomedicine and pharmaceutics. Examples range from the biomedical imaging of articular cartilage [3, 4], micrometastatic lymph nodes [5], breast cancer [6], and porcine burn tissue [7], to the tomographic imaging of transdermal delivery of topically applied drugs [8].

The transdermal drug delivery (TDD) systems, which deliver therapeutically effective amounts of drugs through the skin into the bloodstream, offer many pharmacological advantages over oral and injectable routes, since they enable noninvasive controlled drug delivery and do not require premature hepatic first-pass metabolism [9, 10]. To study TDD pharmacokinetics, the assessment of percutaneous drug permeation is a critical step, and several *in vitro* and *in vivo* methods have been reported. *In vitro* methods estimate chemical diffusion of test substances across an *ex vivo* skin to a fluid reservoir, for example, with the use of Franz diffusion cells followed by high-performance liquid chromatography (HPLC) analysis of the substances [11]. However, such *in vitro* methods are strongly dependent on the environmental conditions such as temperature and humidity [12]. *In vivo* methods measure the percutaneous

*Corresponding author: hhan@postech.ac.kr, ORCID 0000-0002-5101-4416
Color versions of one or more of the figures in this paper are available online.

absorption of drugs by sampling blood or excreta from live animals; however, they require labeling, preferably radio-labeling, of the substances for reliable data [13]. Therefore, there is a strong need for more effective and efficient methods that are noninvasive and enable label-free assessments of the TDD efficiency.

Here we report new, label-free quantitative THz sensing of percutaneous drug permeation, with nicotine patches on human skin as a model TDD system. Nicotine, an addictive chemical component of cigarettes, is well suited for transdermal delivery to help reduce the craving for cigarettes, since it penetrates skin easily. However, the nicotine patch should deliver a prescribed amount over a prolonged period, to avoid overdose symptoms such as irregular heartbeat, nausea, and dizziness [14]. Hence, the transdermal delivery with nicotine patches should be carefully calibrated before their introduction to the market. In this study, by integrating THz-TDS and a semi-analytic approximate model, we demonstrate that transdermal nicotine delivery can be quantitatively assessed without requiring labels (*i.e.*, radioisotopes, fluorophores, *etc.*) and detailed information on the patch's physical and optical features.

II. MATERIALS AND EXPERIMENT

Transmission measurements are performed using a standard THz-TDS system. Briefly, THz pulses are generated using an InAs wafer pumped by a Ti:sapphire laser with a pulse width of 100 fs, and detected by a photoconductive antenna fabricated on a low-temperature-grown GaAs substrate. The THz pulses are collimated and focused by off-axis parabolic mirrors to construct a THz confocal system. To test the sensing capability of our THz-TDS system, a commercial nicotine patch (Nicoderm CQ®, Alza Corp., Vacaville, CA), with a nicotine dose of 7 mg per 24 h (NDC 0067-5124-14) is used. The nicotine patch is a reservoir-type passive TDD system, with a multi-layer structure that consists of a protective backing layer, a nicotine-containing reservoir layer, a rate-controlling membrane, and an adhesive layer (Fig. 1(a), upper panel), according to the manufacturer's specifications [15]. However, detailed material specifications of the commercial nicotine patches, such as structural features (compositions, layer thicknesses, etc.) and optical properties, are not available because they are proprietary information. The patch area and thickness were estimated to be 3×2.5 cm^2 and 250 μm, respectively.

Three nicotine patches are applied to the forearm of a healthy Asian subject (male, 26 years old, 65 kg) and sequentially removed at intervals of 8 h, as shown in the lower panel of Fig. 1(a). The total daily nicotine dose to the subject is 14 mg, which is less than the recommended maximum daily adult dose (21 mg) for smoking cessation by the manufacturer [14]. All experiments are performed in compliance with the guidelines set by the Institutional Biosafety Committee (IBC) at the Pohang University of Science and Technology and were approved by the IBC. THz transmission measurements are carried out for all three patches, removed at the designated intervals, and a fresh patch (control) by placing them on a copper plate with a rectangular aperture, as shown in the lower panel of Fig. 1(b).

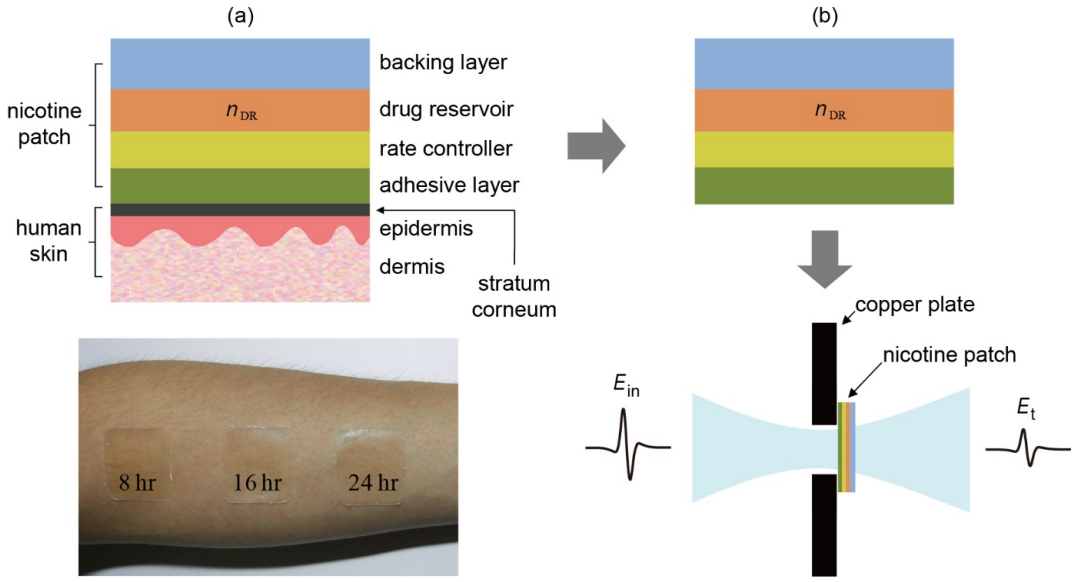

FIG. 1. (a) Cross-sectional schematic of a nicotine patch on human skin (top), and nicotine patches applied to the forearm of an Asian subject (male, 23 years old, 65 kg) (bottom). (b) Cross-sectional schematic of a nicotine patch removed from the skin at a designated time interval (top), and a schematic of a patch mounted on a copper plate with a rectangular aperture for THz transmission measurements.

III. RESULTS AND DISCUSSION

In principle, the transfer matrix method (TMM) [16] could be used for the quantitative analysis of the multi-layer structure in the nicotine patches. However, the TMM analysis requires detailed information about the patches, such as thicknesses and THz refractive indices of the polymer layers, which are not readily available for commercial nicotine patches. Instead, we develop a semi-analytic approximate method and show that the time evolution of the cumulative amounts of nicotine (CAN) can be estimated by using a single-layer model based on an effective medium approximation (EMA) even when information about the properties of materials such as layer thicknesses, structural compositions, and THz properties are not available.

Figure 2 shows the THz transmission signals in the time and frequency domains. The first (single-pass) THz pulses transmitted through the four patches, including the fresh patch, lag the air signal by $t_{01} \approx 0.43$ ps, and the time delay between the first and second (double-pass) THz pulses is $t_{12} \approx 2.43$ ps for all four patches (Fig. 2(a)), indicating that the multilayered structure has a low index contrast. As a result, the internal Fabry-Perot effect due to the multilayered structure is not significant, and the positive peaks of the THz pulses monotonically increase with the application time of the nicotine patch (Fig. 2(a), inset). This implies that the THz absorption by nicotine is reduced as the amount of nicotine in the reservoir layer decreases. During transdermal delivery, the refractive indices of the layers, except for the nicotine-containing layer, should remain relatively constant; thus the effective refractive index n_{eff} of the nicotine patch is given approximately by $n_{\text{eff}} = 1 + ct_{01}/d$, where c is the speed of light in vacuum. Using the measured values for t_{01} and d, n_{eff} is estimated to be ~1.51, which is very close to the THz refractive indices of ~1.5 for nicotine [17] and commonly used plastic films [18]. The patch's structural composition is not available; however, assuming that one of the common polymers is used in the commercial nicotine patches, this strongly supports the validity of the single-layer EMA-based model, since the effect of internal multiple reflections between layers is not significant with low index contrast.

Furthermore, as shown in the inset of Fig. 2(a), the THz transmission coefficient increases at a small rate of about 2% on average for each interval of $\Delta t = 8$ h, indicating a nearly piecewise-linear increase of the THz transmission coefficient with respect to patch application time. Accordingly, we propose a piecewise-linear model for the time evolution of transdermal nicotine delivery

$$T_m = T_0 + \sum_{i=1}^{m} \triangle T_i = T_0 + \sum_{i=1}^{m} A_i \triangle t \,, \tag{1}$$

where T_m is the THz transmission coefficient in the m^{th} time interval ($m = 1, 2, 3$), T_0 is the transmission coefficient for the fresh patch, and ΔT_i is an increment of THz transmission with increment rate $A_i = \Delta T_i / \Delta t$, for the i^{th} time interval (i = 1, 2, 3) of 8 h. Using the piecewise-linear model, we can also define the CAN as

$$M_m = \sum_{i=1}^{m} \triangle M_i = \sum_{i=1}^{m} B_i \triangle T_i \,, \tag{2}$$

where M_m is the total nicotine mass delivered to the blood at the end of the m^{th} time interval (m = 1, 2, 3), and ΔM_i and $B_{\text{i}} = \Delta M_i / \Delta T_i$ are and increment of nicotine mass delivered to blood and the transmission-to-mass conversion factor for the i^{th} time interval ($i = 1, 2, 3$) of 8 h, respectively.

Figure 3 shows the CAN curves calculated on the basis of time-domain (positive peaks of THz pulses) and frequency-domain (spectral amplitudes at 0.4, 0.5, and 0.9 THz) data, as well as the previously reported data with a nicotine dose of 30 mg per 24 h [19] estimated by the conventional *in vitro* and *in vivo* methods, for direct

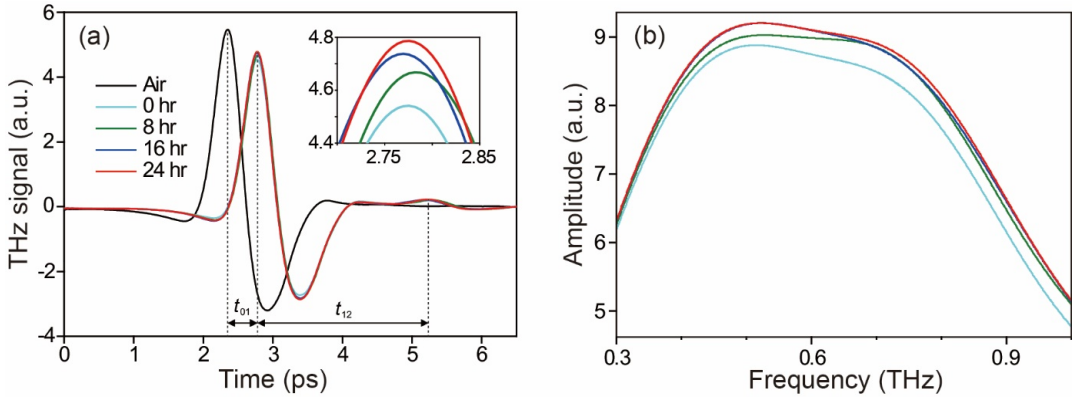

FIG. 2. THz transmission signals, in the (a) time and (b) frequency domains, for air reference (black solid line), a fresh (*i.e.* 0-h) patch (cyan solid line), a patch after 8-h application (green solid line), a patch after 16-h application (blue solid line), and a patch after 24-h application (red solid line).

comparison. Table 1 shows the normalized increments of transmission coefficients, increment rates, transmission-to-mass conversion factors, and CANs in the frequency and time domains used in Fig. 2(b). The results indicate that our THz-TDS data agree well with those of the previously reported conventional methods. In particular, the CAN curve based on time-domain data (red solid line) showed excellent agreement with the results of the conventional methods, and lies between the curves of the conventional *in vitro* (yellow dashed line) and *in vivo* (brown dashed

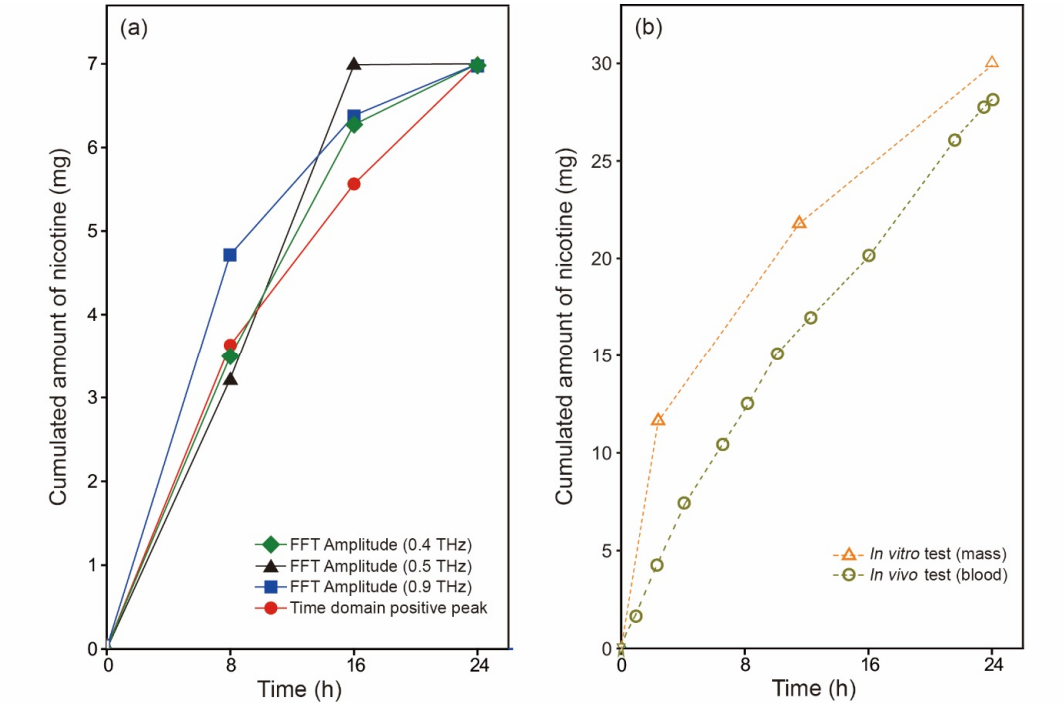

FIG. 3. Cumulative amount of nicotine (CAN) released from (a) the nicotine patches on the basis of spectral amplitude at 0.4 THz (green solid line and solid diamonds), 0.5 THz (black solid line and solid triangles), and 0.9 THz (blue solid line and solid squares), and time-domain positive peaks (red solid line and solid circles) from THz transmission measurements, and (b) previously reported *in vitro* data (yellow dashed line and hollow triangles) and previously reported *in vivo* data (brown dashed line and hollow circles) [19]. Note that a nicotine dose of 7 mg per 24 h is used in this study, but that the *in vitro* and *in vivo* data from [19] are based on nicotine doses of 30 mg per 24 h.

TABLE 1. Parameters used in CAN estimations of nicotine patches

		Time domain (positive peak)	Frequency domain		
			0.4 THz	0.5 THz	0.9 THz
Increment of THz transmission signal	$\triangle T_1/T_0$	0.028	0.015	0.016	0.054
	$\triangle T_2/T_0$	0.015	0.012	0.019	0.019
	$\triangle T_3/T_0$	0.011	0.003	0.00002	0.007
Increment rate (1/hour)	A_1	0.02	0.02	0.02	0.04
	A_2	0.01	0.01	0.02	0.01
	A_3	0.01	0.003	0.00002	0.01
Transmission-to-mass conversion factor (mg^{-1})	B_1	25.29	27.96	26.79	14.38
	B_2	35.60	30.18	18.79	15.04
	B_3	27.42	24.67	45.54	11.86
Cumulated amount of nicotine (CAN) (mg)	M_1	3.21	3.55	3.82	4.74
	M_2	5.68	6.48	6.99	6.52
	M_3	7.00	7.00	7.00	7.00

line) methods.

One notable feature of the THz-TDS measurements is that the CAN curves tend to saturate over time, which is very similar to the results measured by the conventional *in vitro* method for assessing residual nicotine masses in the patches, or by the conventional *in vivo* method for measuring nicotine concentration in the blood. This implies that our THz-TDS-based approach could serve as a viable alternative to the conventional methods, particularly *in vivo* methods, by enabling noninvasive, label-free, and quantitative analyses of the TDD efficiency. However, additional animal and human model studies are necessary for further validation of the efficacy of the THz-TDS-based approach presented in this study, and for its further optimization and generalization to other TDD systems.

IV. CONCLUSION

We performed a label-free THz-TDS to study the transdermal nicotine delivery in commercial nicotine patches on human skin. We developed a piecewise-linear model based on an effective medium approximation to facilitate the quantitative analyses of CAN released from the nicotine patches, without detailed information on their structural and optical properties. The THz-TDS data were in good agreement with measurements by the conventional *in vitro* and *in vivo* methods. Hence, although additional validations are required in more animal and human models, our proposed method has demonstrated high promise for noninvasive and quantitative label-free TDD assessments, further encouraging the exploration of THz-TDS techniques for biomedical, pharmaceutical, and cosmetic applications among many others.

ACKNOWLEDGMENT

This work was supported by the Ministry of Science and ICT (MSIT), Korea, under ICT Consilience Creative program (IITP-2019-2011-1-00783) supervised by the Institute for Information & Communications Technology Planning & Evaluation (IITP).

REFERENCES

1. R. M. Woodward, V. P. Wallace, R. J. Pye, B. E. Cole, D. D. Arnone, E. H. Linfield, and M. Pepper, "Terahertz pulse imaging of *ex vivo* basal cell carcinoma," J. Invest. Dermatol. **120**, 72-78 (2003).
2. S. W. Smye, J. M. Chamberlain, A. J. Fitzgerald, and E. Berry, "The interaction between Terahertz radiation and biological tissue," Phys. Med. Biol. **46**, R101 (2001).
3. E. Jung, H.-J. Choi, M. Lim, H. Kang, H. Park, H. Han, B.-H. Min, S. Kim, I. Park, and H. Lim, "Quantitative analysis of water distribution in human articular cartilage using terahertz time-domain spectroscopy," Biomed. Opt. Express **3**, 1110-1115 (2012).
4. E. Jung, H. Park, K. Moon, M. Lim, Y. Do, H. Han, H. J. Choi, B.-H. Min, S. Kim, I. Park, and H. Lim, "THz time-domain spectroscopic imaging of human articular cartilage," J. Infrared, Millimeter, Teraherz Waves **33**, 593-598 (2012).
5. E.-A. Jung, M.-H. Lim, K.-W. Moon, Y.-W. Do, S.-S. Lee, H.-W. Han, H.-J. Choi, K.-S. Cho, and K.-R. Kim, "Terahertz pulse imaging of micro-metastatic lymph nodes in early-stage cervical cancer patients," J. Opt. Soc. Korea **15**, 155-160 (2011).
6. P. C. Ashworth, E. Pickwell-MacPherson, E. Provenzano, S. E. Pinder, A. D. Purushotham, M. Pepper, and V. P. Wallace, "Terahertz pulsed spectroscopy of freshly excised human breast cancer," Opt. Express **17**, 12444-12454 (2009).
7. Z. D. Taylor, R. S. Singh, M. O. Culjat, J. Y. Suen, W. S. Grundfest, H. Lee, and E. R. Brown, "Reflective terahertz imaging of porcine skin burns," Opt. Lett. **33**, 1258-1260 (2008).
8. K. W. Kim, H. Kim, J. Park, J. K. Han, and J.-H. Son, "Terahertz tomographic imaging of transdermal drug delivery," IEEE Trans. Terahertz Sci. Technol. **2**, 99-106 (2012).
9. J. Wu, K. S. Paudel, C. Strasinger, D. Hammell, A. L. Stinchcomb, and B. J. Hinds, "Programmable transdermal drug delivery of nicotine using carbon nanotube membranes," Proc. Natl. Acad. Sci. U.S.A. **107**, 11698-11702 (2010).
10. M. R. Prausnitz and R. Langer, "Transdermal drug delivery," Nat. Biotechnol. **26**, 1261-1268 (2008).
11. OECD, "Section 4: Health Effects," in *OECD Guidelines for the Testing of Chemicals* (OECD, 2004), Test NO. 428.
12. T. J. Franz, "Percutaneous absorption. On the relevance of *in vitro* data," J. Invest. Dermatol. **64**, 190-195 (1975).
13. OECD, "Section 4: Health Effects," in *OECD Guidelines for the Testing of Chemicals* (OECD, 2004), Test NO. 427.
14. Nicoderm CQ®, *How to use NicoDerm CQ* (Nicoderm CQ®), https://www.nicodermcq.com/about-nicoderm-cq/how-to-use-nicoderm-cq.html (Accessed date: 14 May 2020).
15. Advameg, Inc., *Nicotine patch* (How Products Are Made), http://www.madehow.com/Volume-3/Nicotine-Patch.html#ixzz47mtvWygA (Accessed date: 14 May 2020).
16. S. L. Chuang, *Physics of Photonic Devices*, 2nd ed. (John Wiley&Sons, NJ, USA, 2009), pp. 202-220.
17. B. Yu, Z. Huang, X.-Y. Wang, and G.-Z. Zhao, "Study on THz spectra of nicotinic acid, nicotinamide and nicotine," Spectrosc. Spectral Anal. **29**, 2334-2337 (2009).
18. Y.-S. Jin, G.-J. Kim, and S.-G. Jeon, "Terahertz dielectric properties of polymers," J. Korean Phys. Soc. **49**, 513-517 (2006).
19. S. K. Gupta, N. L. Benowitz, P. Jacob 3rd, C. N. Rolf, and J. Gorsline, "Bioavailability and absorption kinetics of nicotine following application of a transdermal system," Br. J. Clin. Pharmacol. **36**, 221-227 (1993).